An algorithm for fast flexible power point tracking in photovoltaic power plants

Narang, Aditi; Tafti, Hossein Dehghani; Townsend, Christopher D.; Farivar, Glen; Pou, Josep; Konstantinou, Georgios; Vazquez, Sergio

2019

Narang, A., Tafti, H. D., Townsend, C. D., Farivar, G., Pou, J., Konstantinou, G., & Vazquez, S. (2019). An algorithm for fast flexible power point tracking in photovoltaic power plants. IECON 2019 - 45th Annual Conference of the IEEE Industrial Electronics Society. doi:10.1109/IECON.2019.8927083

https://hdl.handle.net/10356/136953

https://doi.org/10.1109/IECON.2019.8927083

An Algorithm for Fast Flexible Power Point Tracking in Photovoltaic Power Plants

Aditi Narang, *Student Member, IEEE,* Hossein Dehghani Tafti, *Member, IEEE,*
Christopher D. Townsend, *Member, IEEE,* Glen Farivar, *Member, IEEE,* Josep Pou, *Fellow, IEEE,*
Georgios Konstantinou, *Senior Member, IEEE,* Sergio Vazquez, *Senior Member, IEEE*

***Abstract*—Flexible power point tracking (FPPT) is control of active power generated by grid-connected photovoltaic power plants (GCPVPPs) to provide various grid-support functionalities, such as frequency response and voltage support. Fast transient response is required during grid voltage and frequency variations. An algorithm, based on dynamic voltage reference design and model predictive control for the dc-dc converter in GCPVPPs is introduced in this paper. The main novelty of the proposed algorithm is fast dynamic response based on the maximum capacity of the system. This feature enables fast FPPT operation in GCPVPPs. The proposed control algorithm results in several features for the FPPT operation, including: higher bandwidth, low power oscillations during steady-state, flexibility for adding constraints based on the operation conditions, and ease of implementation without requiring any complex control parameters tuning and design procedure. The transient performance of the proposed algorithm is evaluated under conditions of voltage sag and frequency deviation. Experimental results are also provided to demonstrate the effectiveness of the proposed algorithm when subjected to rapid changes in PV reference power.**

***Index Terms*—Constant power generation, flexible power point tracking (FPPT), grid connected photovoltaic power plants (GCPVPP), photovoltaic systems, dynamic voltage reference design, model predictive control (MPC)**

I. Introduction

An evolution in the infrastructure associated with photovoltaic (PV) plants has occurred due to the increasing penetration of renewable energy systems, in particular grid-connected photovoltaic power plants (GCPVPPs). There has been a considerable boost in the installation of photovoltaic systems as a result of advancements in PV technology, decline in the price of PV panels and increasing awareness of limited availability of conventional fossil-fuel based energy resources as well as global warming concerns [1].

In a GCPVPP, there are various potential and existing challenges that need to be resolved, which are also critical to the reliability of the power system [2]. For instance, grid codes and standards are continually updated with new requirements such as constant power generation [3], [4]. The aim of this new requirement is to reduce the uncertainty associated with PV power as it changes according to environmental conditions [5], [6]. Additionally, power reserve control [7] and power ramp rate control [8] are mandatory standards applied by GCPVPPs. In order to comply with the new regulations, maximum power point tracking (MPPT) algorithms have been replaced by flexible power point tracking (FPPT) algorithms to enable the flexible power extraction from PV panels according to the grid requirements [6].

The grid codes also regulate voltage support and frequency response for GCPVPPs, in order to enhance the reliability and stability of the power system. These requirements impose fast response capability on GCPVPPs. Therefore, FPPT algorithms with fast response are required. However, the main focus of previous studies was the design of a general algorithm, which calculates the voltage reference of the PV strings, based on the power reference [6]. In order to obtain fast dynamic response and low power oscillations during steady-state, an adaptive voltage-step calculation algorithm was also introduced in [2]. However, the transient response was limited by the bandwidth of the dc-dc converter controller, due to its reliance on conventional proportional-integral (PI) controller. The application of a conventional PI loop for FPPT operation has several drawbacks besides limited bandwidth, including lack of explicit consideration of constraints/saturation in generation of the control output and tedious tuning requirements [9], [10].

To tackle the above mentioned drawbacks, an algorithm based on the dynamic voltage reference design is introduced in this paper. The main novelty of the proposed approach is to use the maximum capacity of the power converter to track the voltage reference under transients. This is achieved by calculating the inductor current reference based on the voltage reference provided by the FPPT algorithm and system parameters. A model-predictive based controller is also proposed to regulate the average current of the inductor of the boost converter, to the calculated value with the dynamic voltage reference algorithm. Another advantage of the proposed algorithm is the capability of adaptively changing the maximum saturation of the inductor current, based on the inverter operation to avoid mismatching the power between the dc-dc converter and inverter, even during transients. Furthermore,

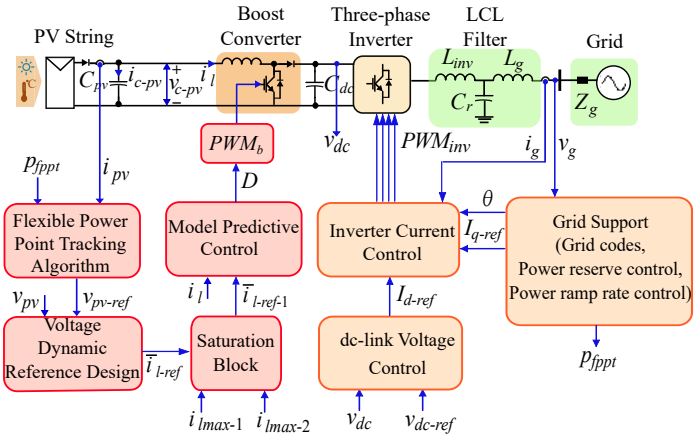

Fig. 1. Circuit configuration and overall control structure of the two-stage GCPVPPs.

the design of the proposed controller is straightforward and it does not contain tuning complexities, which exist in conventional controllers. Simulation results are provided to verify the performance of the proposed fast FPPT algorithm under grid voltage sag condition and frequency increase. Furthermore, the transient performance of the proposed algorithm is verified using a 1 kW two-stage GCPVPP experimental setup.

The structure of the paper is as follows: the details of the proposed dynamic reference-based fast FPPT algorithm are provide in Section II. The performance of the proposed algorithm under voltage sag and frequency decrease in the grid is evaluated using simulation and results are presented in Section III. The experimental results on a down-scaled prototype are provided in Section IV, and the conclusions of the study are presented in Section V.

II. Proposed Control Algorithm

The circuit configuration of a two-stage GCPVPP is depicted in Fig. 1. The controller is divided in two parts, as follows:

A. Controller of the Grid-connected Inverter

The grid-connected inverter provides grid support functionalities, like power reserve control and voltage control. It also regulates the dc-link voltage to its reference value by calculating the d-axis current reference $I_{d\text{-}ref}$. During voltage sag conditions, the q-axis current reference, $I_{q\text{-}ref}$ is calculated based on the grid voltage as shown below [11]:

$$I_{q\text{-}ref} = \begin{cases} 0 & 0.9 \leq \hat{V}_{min} < 1.1 \\ k\frac{\triangle V}{\hat{V}_N} I_{Ndq} + I_{q0} & 0.5 \leq \hat{V}_{min} < 0.9 \\ -I_{Ndq} + I_{q0} & \hat{V}_{min} < 0.5, \end{cases} \quad (1)$$

where, $\hat{V}_N$ denotes the normalized amplitude of the grid phase voltage, $\triangle V = \hat{V}_{min} - \hat{V}_N$ and $\hat{V}_{min}$ is the value of minimum phase voltage. I_{Ndq} denotes the peak inverter current in dq-frame. I_{q0} is the initial q-axis current, prior to voltage sag occurrence. k is a constant whose value is based on the agreement between the grid operators and GCPVPP owners [12]. It is considered to be 2 in this study. Equation 1 shows the formula for calculation of q-axis reference current for any type of voltage sag occurring in the system. The given formula is generalized for single phase, bi-phase or even a three phase voltage sag. During the normal condition, when the voltage is within the allowable range, no reactive current or power needs to be injected into the grid. When the voltage range is between 0.9 and 0.5, the q-axis current reference depends on the minimum grid voltage value, whereas when the voltage dips below 0.5 p.u, the current injected into the grid is purely reactive. The direct and quadrature axis reference currents are converted to the abc-frame using the inverse park transformation. The resulting grid reference currents are used in the inverter current controller in order to regulate the grid currents.

In addition to the voltage support, the GCPVPPs should provide frequency response capability. The frequency response grid requirements for different countries are depicted in Fig. 2. While the grid frequency is within the frequency control band (f_2 and f_3), a power reserve value of ΔP is considered between the extracted PV power and its maximum available power. This enables the GCPVPP to increase the output power to maximum available power (P_{avai}), if the grid frequency drops below f_2. If the frequency is between f_1 and 47 Hz, the PV injects the maximum power P_{avai} to the grid. On the other hand, for frequencies larger than the upper limit of the frequency band f_3, the PV power reduces based on the droop gain, given in the standard. While the grid frequency is larger than 52 Hz, the PV power reduces to zero ad the PV system disconnects from the grid. There is no time limit on how fast the system should respond to grid frequency

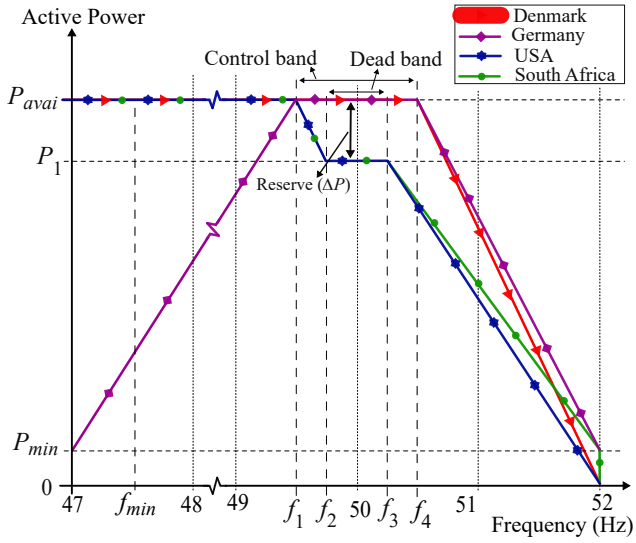

Fig. 2. Frequency support regulations by international grid codes.

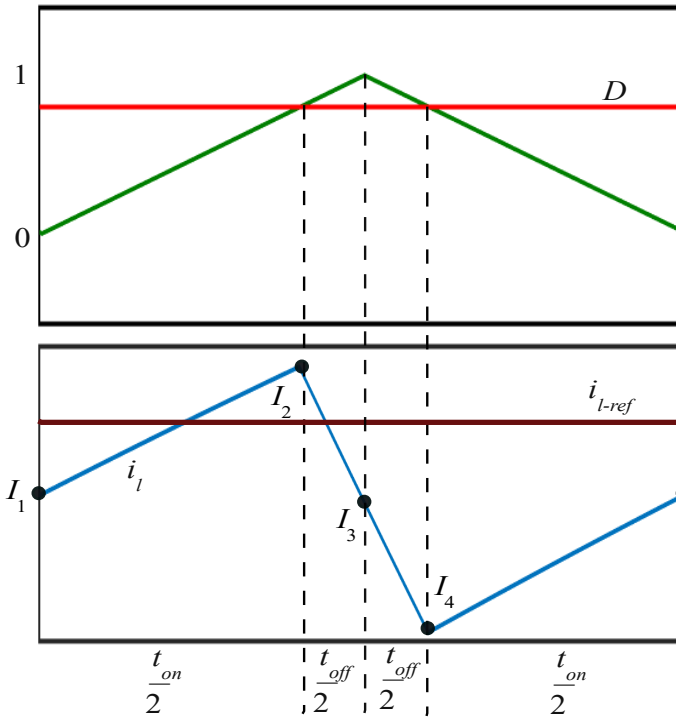

violation, however, a quick response would ensure better reliability of the system.

B. Proposed Fast FPPT Control Algorithm for the dc-dc Converter

As shown in Fig. 1, according to the inverter current limitations and grid requirements for the control of the injected active power to the grid, the active power reference p_{fppt}, to be extracted from the PV strings is calculated [13]. The power reference p_{fppt} is then used by the FPPT algorithm to calculate the PV voltage reference, $v_{pv\text{-}ref}$. In this study, an adaptive FPPT algorithm based on [2], is implemented to achieve fast dynamics in order to reach the steady state.

The PV voltage reference $v_{pv\text{-}ref}$, calculated with the FPPT algorithm is provided as the input to the dynamic voltage reference design, in order to calculate the inductor average current reference, $\bar{i}_{l\text{-}ref}$. The dynamic voltage reference design was first introduced for active front-end rectifiers [10]. The main idea is to restrict the increment of the PV voltage v_{pv} to N steps. In order to achieve fast response under transient conditions, the parameter N should be fixed at a value of 1. In this condition, the maximum capacity of the converter can be used to track the voltage reference during transients [9].

The inductor average current reference $\bar{i}_{l\text{-}ref}$ can be calculated based on the calculated PV voltage reference $v_{pv\text{-}ref}(k)$ in each calculation-step. The PV capacitor C_{pv} current ($i_{c\text{-}pv}$), in Fig. 1, is calculated as

$$i_{c\text{-}pv} = C_{pv}\frac{dv_{c\text{-}pv}}{dt} = \frac{C_{pv}\left[v_{c\text{-}pv}(k+1) - v_{c\text{-}pv}(k)\right]}{T}, \quad (2)$$

where $v_{c\text{-}pv}(k)$ and $v_{c\text{-}pv}(k+1)$ are the PV capacitor voltages at instances k and $k+1$, respectively. The aim of the

TABLE I
SIMULATION PARAMETERS

Symbol	Quantity	Values
$V_{g\text{-}rms}$	Grid voltage (rms value)	220 V
C_{pv}	PV capacitor	1.5 mF
L	Boost inductance	3 mH
V_{dc}	dc-link voltage	600 V
f_s	Switching frequency	15 kHz
f_g	Grid frequency	50 Hz
P_{mpp}	Maximum Power	2.3 kW
I_{mpp}	Current at maximum power point	14.7 A
V_{mpp}	Voltage at maximum power point	160 V

current using MPC algorithm, all the variables that the current to be regulated depends upon are measured for the current time step. The computation of the duty cycle corresponding to the next switching period requires the values of these variables in the present switching cycle. The main aim of this algorithm is to minimize the error between the inductor current reference, $\bar{i}_{l\text{-}ref}$ and the average inductor current. The inductor current waveform in the steady state is shown in the Fig. 3. The calculated inductor current reference value used to find the duty ratio is shown in the following relation:

$$\bar{i}_{l\text{-}ref} = D\frac{(I_1+I_2)}{4} + (1-D)\frac{(I_2+I_3)}{4} + (1-D)\frac{(I_3+I_4)}{4} + D\frac{(I_4+I_5)}{4} \quad (6)$$

The current values I_1, I_2, I_3, I_4 and I_5 as indicated in Fig. 3 can be found out by computational analysis.

I_1 and I_5 are calculated during t_{on}, whereas I_3 is calculated during t_{off}, and I_2 and I_4 are calculated on the edge of on and off periods of the duty cycle. The duty ratio, D is calculated from (7)

$$D = \frac{\bar{i}_{l\text{-}ref} - i_l + \frac{T}{L}(v_{c\text{-}pv} - v_{pv})}{\frac{Tv_{pv}}{L} + \frac{T}{L}(v_{c\text{-}pv} - v_{pv})} \quad (7)$$

Finally, the switching signal for the dc-dc boost converter is generated via carrier-based pulse-width modulation, from the duty cycle which is calculated by the model predictive control algorithm.

III. SIMULATION RESULTS

The performance of the proposed algorithm is evaluated by simulating voltage sag and frequency deviation conditions in Matlab/Simulink software. The parameters of the simulation setup are presented in Table I.

Case I: The performance of the proposed fast FPPT algorithm under grid voltage sag is evaluated in this case study and results are shown in Fig. 4. There is a voltage sag in phases B and C, with the minimum amplitude of $0.6\,\mathrm{p.u}$ at at $t = 0.2\,\mathrm{s}$,. As observed from Fig. 4(d), the PV power reference $p_{pv\text{-}ref}$ drops from $2.5\,\mathrm{kW}$ to around $1\,\mathrm{kW}$, according to (1). Consequently, the proposed fast FPPT algorithm reduces the PV voltage to around $60\,\mathrm{V}$ in less than $0.2\,\mathrm{s}$as is seen in Fig. 4(b). It should be noted that the operation point of the PV strings is considered to be in the left-side of the maximum power point (MPP) in this case study. It is seen that at every step change of the PV voltage, the inductor current reaches its maximum value or zero, which implies the application of the maximum capacity of the converter in tracking the voltage reference under transients. This feature enables reducing the time-step and increasing the voltage-step of the FPPT algorithm, which results in fast FPPT operation. Since, the voltage sag is within the range of $0.5\,\mathrm{p.u.}$ and $0.9\,\mathrm{p.u.}$, both active and reactive powers are injected into the system as per (1) and shown in Fig. 4(e). This case study shows the fast dynamic response of the proposed control algorithm under grid voltage sags.

Case II: A drop in frequency occurs if the power demand exceeds the supply power. This case study shows the dynamic response of the proposed algorithm in case of the frequency deviations in the grid and results are shown in Fig. 5. Due to the decrease of the grid frequency from $50\,\mathrm{Hz}$ to $48.5\,\mathrm{Hz}$, the PV power reference $p_{pv\text{-}ref}$ rises from $2\,\mathrm{kW}$ to $2.4\,\mathrm{kW}$, as shown in Fig. 5(d). Since the operating point is on the left-side of the MPP, with increase in PV power, the PV voltage also rises, which can be observed in Fig. 5(b). The PV voltage and power, both converge to their final reference value in less than $0.2\,\mathrm{s}$, thus verifying the fast transient response of the proposed algorithm in order to obtain the fast FPPT operation.

TABLE II
EXPERIMENTAL SETUP PARAMETERS

Symbol	Quantity	Values
$V_{g\text{-}rms}$	Grid voltage (rms value)	80 V
C_{pv}	PV capacitor	180 μF
L	Boost inductance	5 mH
V_{dc}	dc-link voltage	250 V
f_s	Switching frequency	15 kHz
f_g	Grid frequency	50 Hz
P_{mpp}	Maximum Power	1 kW
I_{mpp}	Current at maximum power point	7 A
V_{mpp}	Voltage at maximum power point	140 V

IV. EXPERIMENTAL VERIFICATION

The experimental verification of the proposed algorithm is implemented on a $1\,\mathrm{kVA}$ laboratory setup. The parameters of the system used in the experimental setup are shown

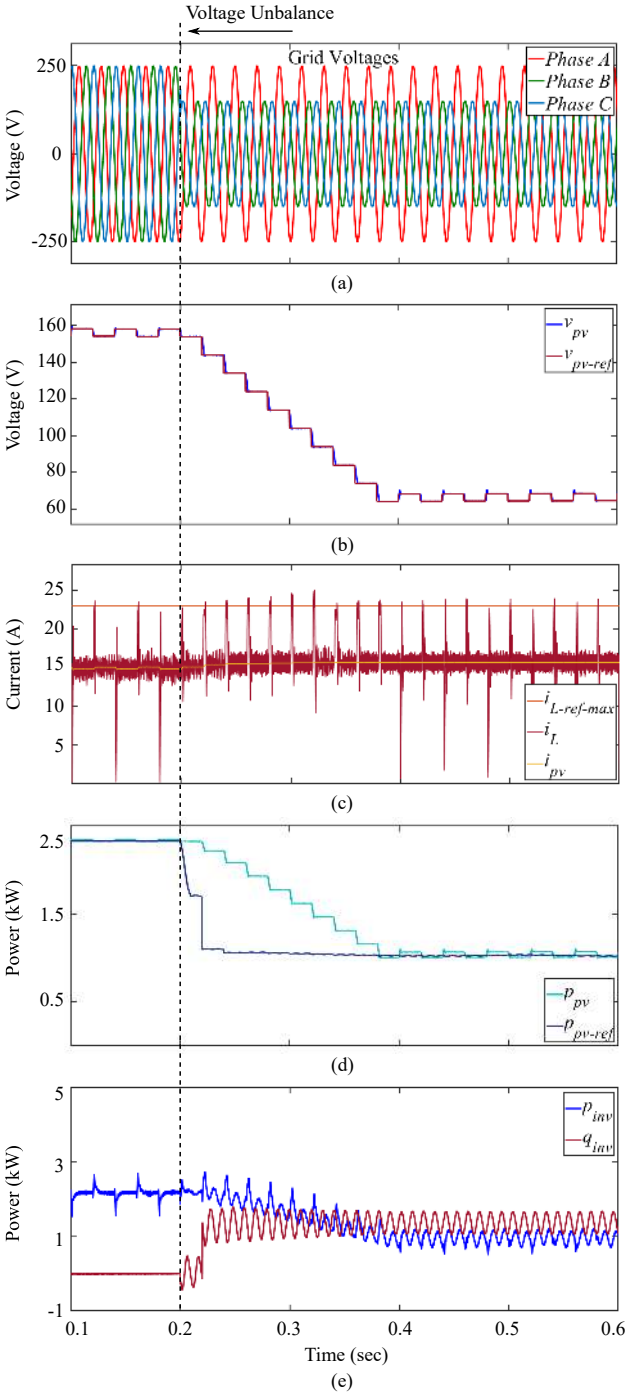

Fig. 4. *Case I*: Verification of the performance of proposed algorithm under voltage sag: (a) Grid voltages, (b) PV voltage and PV reference voltage, (c) inductor and PV current, (d) PV power and PV power reference, and (e) inverter active and reactive powers

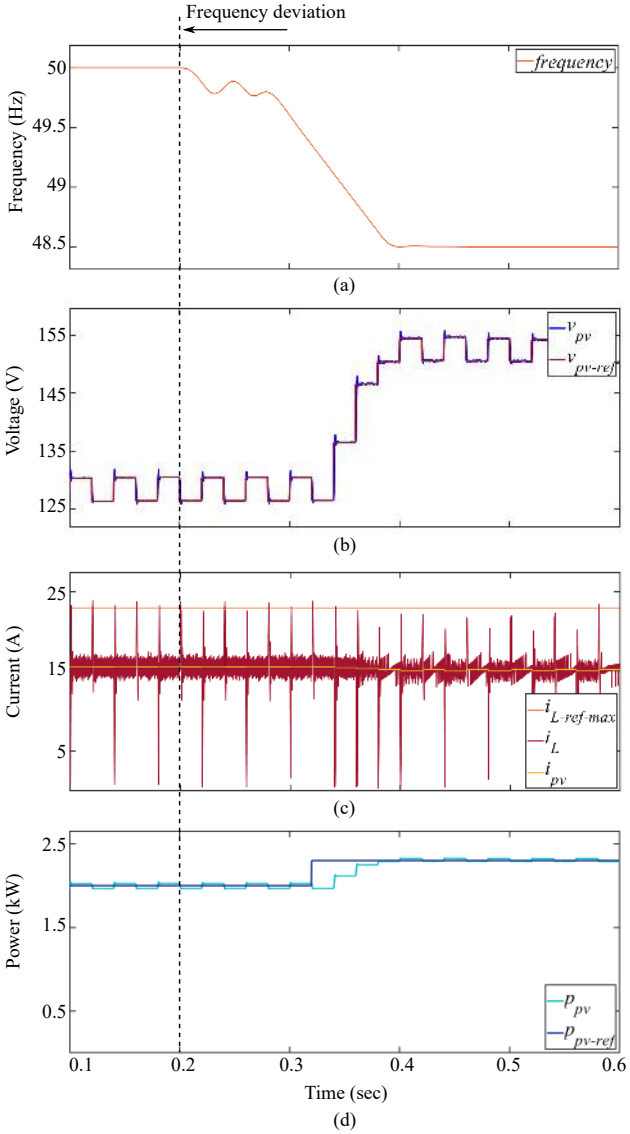

Fig. 5. *Case II*: Verification of the performance of proposed algorithm under frequency deviation, from 50 Hz to 48.5 Hz, when the operating point is on the left side of PV curve: (a) frequency, (b) PV voltage and PV reference voltage, (c) inductor and PV current and reference and, (d) PV power and PV reference power

in Table II. The performance of the proposed algorithm is evaluated under a step-change of the PV reference power $p_{pv\text{-}ref}$. Sudden changes in the grid requirements might take place resulting in rapid changes in PV reference power. Such variations take place upon changes in load demand from the grid. The effect of this change is shown on the power, voltage and current characteristics. There is a rapid increase in the power reference $p_{pv\text{-}ref}$. As seen in Fig. 6, the change in the power reference takes place from 550 W to 950 W. The operation point of the solar power plant lies on the right-hand side of the MPP. Hence, the operating point shifts upwards as the power increases and the PV voltage decreases. It can be seen from Fig. 6 that the response is decently fast as the PV power converges to its new reference value in very small time interval. It takes approximately 0.08 s for the system to get back to its steady state operation.

On the right-hand side, the slope of the PV curve falls with a faster rate than on the left side, and thus, the response is also faster when the operating point lies on the right-hand side of PV curve as is shown in Fig. 6. The PV voltage and inductor current indicated in Fig. 6 and are also observed to reach the steady state within a short time interval.

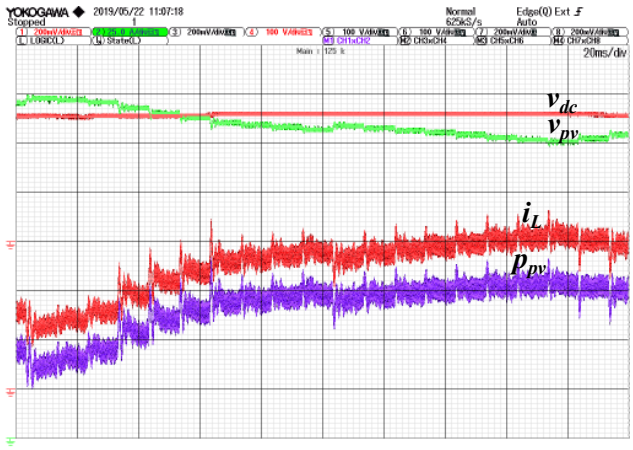

Fig. 6. Experimental verification of the performance of the control algorithm under a change of the PV power reference from 550 W to 950 W, when the operation point is on the right-side of the MPP, showing the PV power, PV voltage, and inductor current.

V. Conclusion

A method to control the dc-dc converter of GCPVPPs has been introduced in this paper. The proposed algorithm uses dynamic voltage reference design as the voltage control technique and calculates the average inductor current reference, and uses the model predictive control to regulate the current and to calculate the duty cycle of the dc-dc converter. The applicability and effectiveness of the proposed technique have been demonstrated by the simulation and experimental results. Fast dynamic response is achieved under a change in the PV reference power and under unbalanced grid voltage condition. The proposed control scheme is sought to be a more flexible method that produces faster transient performance with satisfactory steady state response. The results show considerably small settling time and renders this technique especially effective and adaptive for GCPVPPs, under dynamically changing grid and environmental conditions.

VI. Acknowledgment

This work was supported by the Singapore Ministry of Education Academic Research Fund Tier 1 under Grant No: 2019-T1-001-168.

References

[1] Y. Yang, F. Blaabjerg, and Z. Zou, "Benchmarking of grid fault modes in single-phase grid-connected photovoltaic systems," *IEEE Trans. on Ind Appl.*, vol. 49, pp. 2167–2176, Sep. 2013.

[2] H. D. Tafti, A. Sangwongwanich, Y. Yang, J. Pou, G. Konstantinou, and F. Blaabjerg, "An adaptive control scheme for flexible power point tracking in photovoltaic systems," *IEEE Trans. Power Electron.*, vol. PP, pp. 1–1, Sep. 2018.

[3] R. G. Wandhare and V. Agarwal, "Precise active and reactive power control of the pv-dgs integrated with weak grid to increase PV penetration," in *Proc. IEEE 40th Photovoltaic Specialist Conf. (PVSC)*, pp. 3150–3155, Jun. 2014.

[4] "Technical regulation 3.2.2 for PV power plants with a power output above 11 kW," *Energinet.dk, Errits, Denmark, Document No.: 14/17997-39, Tech. Rep.*, 2015.

[5] A. Sangwongwanich, Y. Yang, and F. Blaabjerg, "High-performance constant power generation in grid-connected pv systems," *IEEE Trans. Power Electron.*, vol. 31, pp. 1822–1825, Mar. 2016.

[6] H. D. Tafti, A. I. Maswood, G. Konstantinou, J. Pou, and F. Blaabjerg, "A general constant power generation algorithm for photovoltaic systems," *IEEE Trans. Power Electron.*, vol. 33, no. 5, pp. 4088–4101, May 2018.

[7] A. Sangwongwanich, Y. Yang, and F. Blaabjerg, "A sensorless power reserve control strategy for two-stage grid-connected PV systems," *IEEE Trans. Power Electron.*, vol. 32, pp. 8559–8569, Nov. 2017.

[8] M. Chamana, B. H. Chowdhury, and F. Jahanbakhsh, "Distributed control of voltage regulating devices in the presence of high PV penetration to mitigate ramp-rate issues," *IEEE Trans. Smart Grid*, vol. 9, pp. 1086–1095, Mar. 2018.

[9] S. Vazquez, A. Marquez, R. Aguilera, D. E. Quevedo, J. I. Leon, and L. G. Franquelo, "Predictive direct power control for grid connected power converters with DC-link voltage dynamic reference design," in *Proc. IEEE Intern. Conf. Ind. Tech. (ICIT)*, pp. 2327–2332, Mar. 2015.

[10] D. E. Quevedo, R. P. Aguilera, M. A. Perez, P. Cortes, and R. Lizana, "Model predictive control of an AFE rectifier with dynamic references," *IEEE Trans. Power Electron.*, vol. 27, pp. 3128–3136, Jul. 2012.

[11] H. D. Tafti, A. Maswood, G. Konstantinou, J. Pou, K. Kandasamy, Z. Lim, and G. H. P. Ooi, "Study on the low-voltage ride-thorough capability of photovoltaic grid-connected neutral-point-clamped inverters with active/reactive power injection," *IET Renewable Power Generation*, vol. 11, no. 8, pp. 1182–1190, Jul. 2017.

[12] Y. Yang, P. Enjeti, F. Blaabjerg, and H. Wang, "Wide-scale adoption of photovoltaic energy: Grid code modifications are explored in the distribution grid," *IEEE Ind Appl. Mag.*, vol. 21, pp. 21–31, Sep. 2015.

[13] H. D. Tafti, A. I. Maswood, G. Konstantinou, J. Pou, and P. Acuna, "Active/reactive power control of photovoltaic grid-tied inverters with peak current limitation and zero active power oscillation during unbalanced voltage sags," *IET Power Electron.*, vol. 11, no. 6, pp. 1066–1073, May 2018.

[14] D. Draghici, M. Gurbina, A. Ciresan, and D. Lascu, "Predictive leading-edge modulation average current control in dc-dc converters," in *Proc. Intern. Conf. on Optim. of Electrical and Electron. Equipment (OPTIM)*, pp. 588–594, May 2014.

[15] P. Cortes, M. P. Kazmierkowski, R. M. Kennel, D. E. Quevedo, and J. Rodriguez, "Predictive control in power electronics and drives," *IEEE Trans. Ind. Electron.*, vol. 55, pp. 4312–4324, Dec. 2008.

[16] T. Geyer, G. Papafotiou, R. Frasca, and M. Morari, "Constrained optimal control of the step-down DC-DC converter," *IEEE Trans. Power Electron.*, vol. 23, pp. 2454–2464, Sep. 2008.

[17] Y. Xie, R. Ghaemi, J. Sun, and J. S. Freudenberg, "Implicit model predictive control of a full bridge DC-DC converter," *IEEE Trans. Power Electron.*, vol. 24, pp. 2704–2713, Dec. 2009.

[18] S. Vazquez, J. I. Leon, L. G. Franquelo, J. Rodriguez, H. A. Young, A. Marquez, and P. Zanchetta, "Model predictive control: A review of its applications in power electronics," *IEEE Ind Electron. Mag.*, vol. 8, pp. 16–31, Mar. 2014.

[19] S. Vazquez, J. Rodriguez, M. Rivera, L. G. Franquelo, and M. Norambuena, "Model predictive control for power converters and drives: Advances and trends," *IEEE Trans. on Ind. Electron.*, vol. 64, pp. 935–947, Feb 2017.

[20] A. Linder and R. Kennel, "Model predictive control for electrical drives," in *Proc. IEEE 36th Power Electron. Specialists Conf.*, pp. 1793–1799, Jun. 2005.

[21] S. Mariethoz, A. Domahidi, and M. Morari, "Sensorless explicit model predictive control of permanent magnet synchronous motors," in *Proc. IEEE Intern. Electric Machines and Drives Conf.*, pp. 1250–1257, May 2009.